MAPPING AIR TEMPERATURE BY FOURIER ANALYSIS OF LAND SURFACE TEMPERATURE TIME SERIES OBSERVED BY TERRA/MODIS

Silvia Maria Alfieri[1], Francesca De Lorenzi[1], Antonello Bonfante[1], Angelo Basile[1]and Massimo Menenti[2]

1. National Research Council, Institute for the Agricultural and Forest System of the Mediterranean, Ercolano (NA), Italy; Silvia.alfieri@isafom-cnr.it
2. Delft University of Technology, Department of Geoscience and Remote Sensing, Delft, The Netherlands; M.menenti@tudelft.nl

ABSTRACT

Mapping Air Temperature at fine spatial resolution is necessary in a wide range of environmental applications including agronomical studies related to climate change. In this work a method for mapping maximum air temperature at 1 km resolution was developed and applied by time series analysis of Land Surface Temperature observed by Terra Moderate-resolution Imaging Spectroradiometer from 2000 to 2006. Land Surface Temperature time series was processed using the Harmonic ANalysis of Time Series algorithm to remove cloud contaminated observations. Successively the output is used to characterize the spatio-temporal pattern of Land Surface Temperature and to determine its interannual variability. We conclude that the interannual variability of the Land Surface Temperature spatial – temporal pattern could be neglected in the analysed period. This result makes possible the use of the average daily temporal trend to downscale Air Temperature data at any period of time with only a limited number of Air Temperature data measured at sparse reference stations. The procedure was tested in the same period of MODIS observations and in a completely independent period of time. The validation against data observed at stations produce RMSE errors less than 3 K.

INTRODUCTION

Air temperature (AT) is the main input to model crop growth, evapotranspiration and soil water stress. High spatial resolution of climate data is necessary for any study of land surface climate, especially when the complexity of the territory has a determinant role in determining the microclimate. This is the case of Valle Telesina, a topographically complex region where the spatial distribution of agricultural crops is largely influenced by local climate. Moreover, a relevant limit in this area is the scarce availability and arbitrary location of meteorological stations to get information about air temperature and its spatial pattern. In these cases, conventional methods for temperature interpolation (i.e. Ordinary Kriging, Inverse Distance Weighting) are often not adequate to capture the range of spatial variability within the area.

Several studies have been carried out by correlation analysis of time series data on air temperature measured at ground and satellite. In one study the temperature-vegetation index method (TVX) has been used, based on the correlation between the vegetation indexes NDVI and air temperature (1, 2). The limited applicability of this method was demonstrated in a work of Vacutsem et al, 2010 (3) where a scarce correlation between the difference of air temperature to surface temperature and NDVI was found. Then, air temperature estimated by the TVX method could be inaccurate or biased depending on the study area. Instead, a strong correlation was already observed and analyzed in previous works between land surface temperature (LST) and air temperature (4, 5, 6). Satellite remote sensing LST has been widely used to map air temperature (7, 8).

The objective of this work is the analysis of LST time series observed by satellite to gain information on time average spatial distribution of air temperature over a certain area. This analysis is used to successively downscale air temperature data. Once assessed the interannual stability of the LST spatial pattern, air temperature downscaling is also possible over time periods different than that analyzed if air temperature measurements are available at least at one location. Spatial pattern of LST are characterized by normalizing LST to a reference point and then processed by Fast Fourier Transform (FFT) analysis to verify interannual stability.

METHODS

A procedure was developed and applied to map air temperature at fine spatial resolution combining analysis of land surface temperature observed by satellite and air temperature measurements at a reference location. Figure 1 shows the work-flow of the procedure.

We implemented and evaluated the algorithm on data collected in the Valle Telesina area to downscale maximum air temperature to 1 km resolution. The air temperature at the reference location is a dataset available on the entire Italian territory at 35 km resolution grid. It has been produced by CRA-CMA within the Italian project "Agroscenari". The dataset spans the period from 1980 to 2009.

Daily LST from Terra MODIS satellite (MOD11A1 product) was used for our implementation. In particular we used the daily overpass data of the Terra satellite from 1 February 2000 to 31 December 2006. Time of LST data sampling is about 12:30 a.m. that could be assumed with good approximation to be the time of maximum air temperature. Moreover Mostovoy et al. 2006 (9) showed that the effect of the difference between the satellite overpass time and the time when maximum air temperature is observed at ground station does not alter the correlation coefficients of the linear regression of LST vs Tair. MODIS LST products are corrected for the atmospheric effects using a split-windows algorithm (10). The error in LST retrieval has been estimated to be about 1 K.

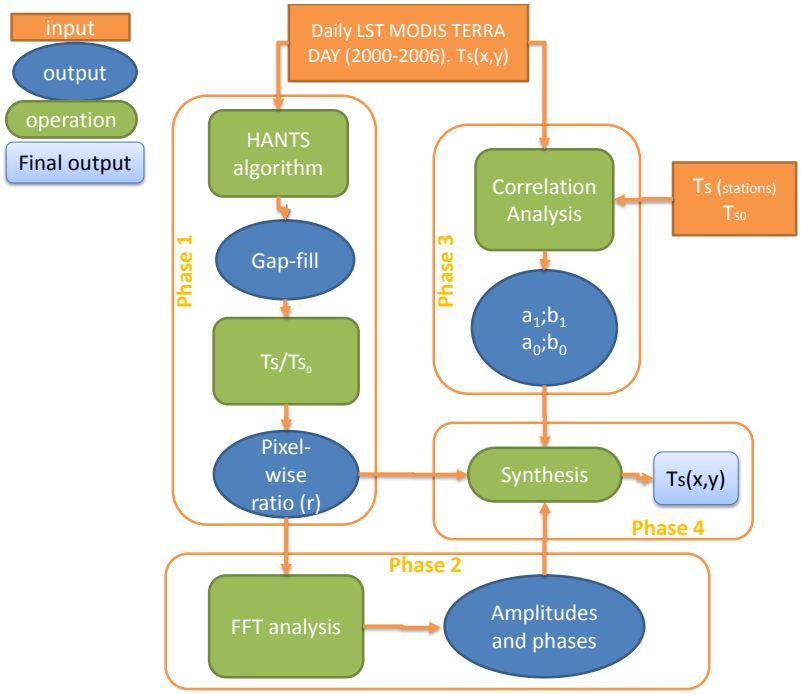

Figure 1. Work-flow of the procedure

Phase 1: Cloud removal and gap filling of LST images and characterization of spatio-temporal patterns.

Cloud removal and gap-filling of LST time series has been performed by Harmonic ANalysis of Time Series (HANTS) algorithm (11, 12). The algorithm handles the Fourier Analysis as curve fitting in iterative steps. Outliers are identified at each step as observations deviating by more than a pre-defined threshold value from the curve fitted at previous step. They are weighted as zero in the subsequent curve fitting process. The iterations continues until all data in time series are within the maximum error (FET: the threshold) or when the number of data points is insufficient to repeat the process (DOD: minimum number of valid observations).

The signal is modelled using a Fourier series:

$$y(t) = \left[a_0 + \sum_{1}^{nf} a_i \cos\left(2\pi f_i t_y\right) + b_i sen\left(2\pi f_i t_y\right) \right]; \quad (1)$$

where nf is the number of frequencies, a_0 is the average of the series, the coefficients a and b are the coefficient of trigonometric components of the frequency j.

We set FET = 8 K and DOD = 50. The reconstructed land surface temperature time series has been normalized to a reference location to characterize spatial patterns. The pixel-wise ratio of surface temperature to that at reference location (*r*) was calculated for the entire time series.

Phase 2: Evaluating interannual stability of r ratio

Harmonic analysis was performed for each year separately to evaluate the interannual stability of the ratio *r*. For the period from 2000 to 2006 the yearly time series of *r* was decomposed by Fourier analysis in the tree main periodic signals with periods respectively of 365, 180 and 120 days. We have then assessed the interannual variability of the amplitude and phase values.

Phase 3: Correlation analysis between air temperature and surface temperature.

Correlation analysis between the air temperature measured at five stations over the area and land surface temperature observed by satellite was performed to find the following relation:

$$T_{air} = T_s * m_1 + n_1 \quad (2).$$

that identifies the equation representative of the entire area. The employed dataset includes daily maximum air temperature data from 2000 to 2006 for each considered station (Regional meteorological network).

The inverse regression is required at the reference location where, since when using the downscaled air temperature in a different climate period (no satellite data available), we only know the air temperature.

$$T0_{air} = T0_s * m_0 + n_0 \quad (3)$$

Phase 4: Air temperature calculation

Daily air temperature at each pixel location was estimated by :

$$Tair(x, y) = \left[\left(T0_{air} * m_0 + n_0\right) * r(x, y)\right] * m_1 + n_1 \quad (4)$$

with $T0_{air}$ is the air temperature at the reference location.

The ratio *r* is calculated as

$$r(x, y) = a_0 + \sum_{1}^{3} a_i \cos(2\pi f_i t_y) + b_i sen(2\pi f_i t_y) \quad (5)$$

where

$$a = \overline{A} * \cos(\overline{\psi} * \frac{\pi}{180}); \quad b = \overline{A} * sen(\overline{\psi} * \frac{\pi}{180}); \tag{6}$$

where $\overline{A}$ and $\overline{\psi}$ are respectively the amplitude and phases averaged over the period from 2000 to 2006, once the interannual stability of the ratio has been verified.

RESULTS

The analysis of time series with HANTS requires some preliminary analysis of the data to find the best set of parameters, particularly which frequencies to consider for modelling the time series and the target error (FET). The annual trend of land surface temperature averaged over the period 2000-2006 (Figure 2 show an example at one pixel location) suggests that uni-modal temporal profile is characteristic of the entire scene. This can be described using the three frequencies with period 365, 180 and 120 days. The time series of land surface temperature was processed using the HANTS algorithm on a yearly basis.

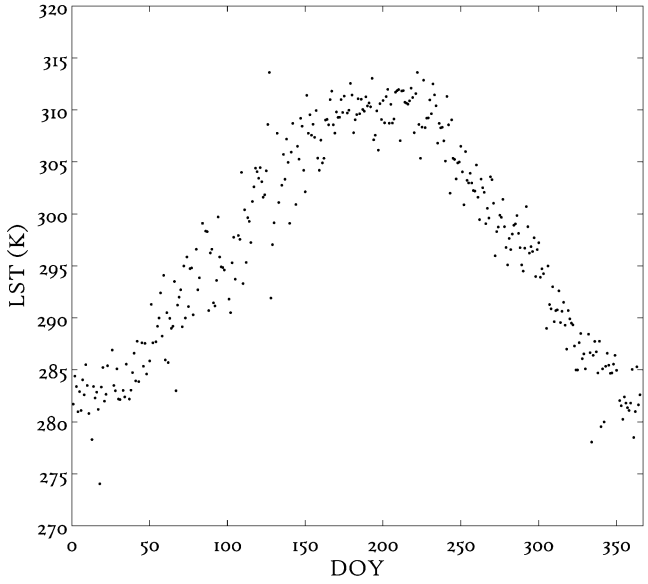

Figure 2. Mean values over 2000-2006 of daily land surface temperature measured by MODIS/TERRA satellite at one pixel location.

The spatial pattern of LST on any given day was characterized by the ratio *r* using reconstructed surface temperature values. At each pixel the *r* ratio shows a periodical trend that is determined by the seasonality of net radiation and of its allocation to sensible and latent heat flux. These factors have a significant spatial variability due to soil moisture, altitude, exposure, slope and land cover. Figures 3a and 3b show the typical spatial pattern in summer and winter seasons. The lower radiative forcing during the winter season is reflected in a reduced spatial variability than in summer.

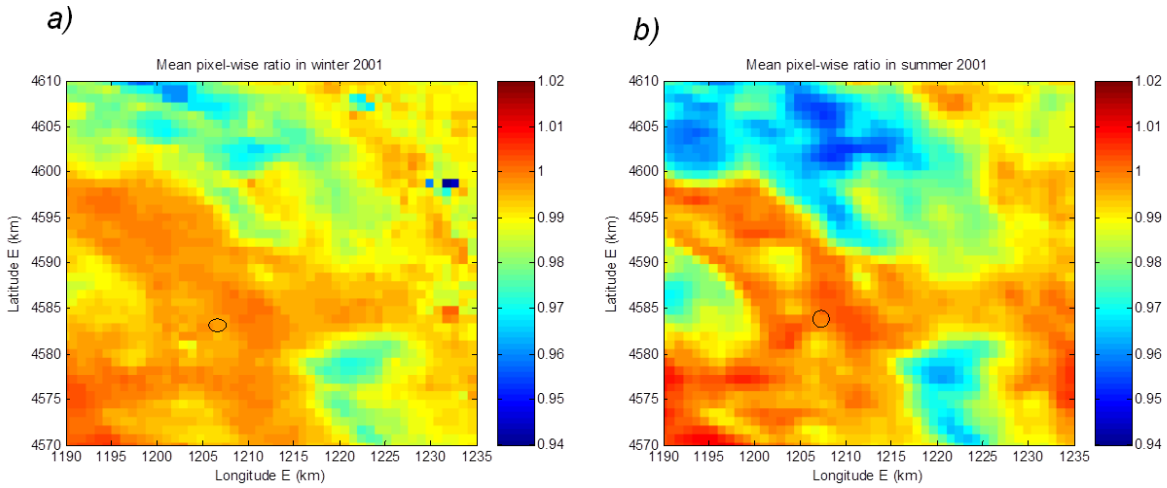

Figure 3. Maps of mean values of r ratio in Winter (a) and in Summer (b) seasons. The black circle indicates the position of the reference point.

The interannual variability of pixel-wise ratio *r* has been evaluated by the calculation of coefficient of variation (*cv*) of the amplitudes at the period 365, 180 and 120 days. Figure 4 show the map of *cv* for the first harmonic amplitude.

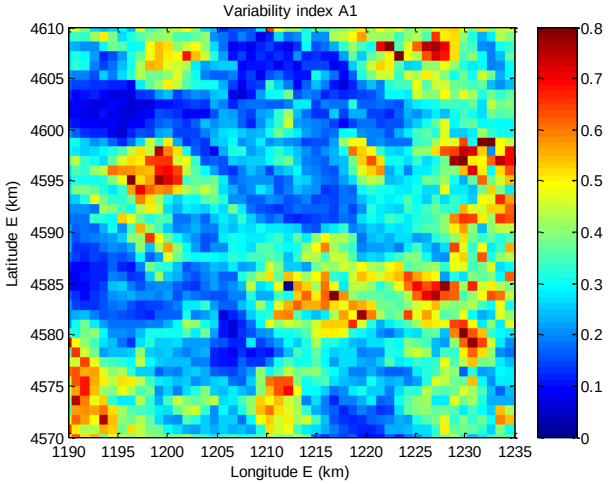

Figure 4. Coefficient of variation of the first harmonic amplitude (period =365 days).

Table 1 shows the coefficient of variations of the amplitudes of the three harmonic components multiplied by the corresponding amplitude. This product is a measure of the inter-annual variability and it indicates that we can neglect such variability, since these products are much smaller than the mean value of r.

Table 1. Product of cv to mean values of the amplitudes over Valle Telesina area compared with area average value of r

cv_A1*A1	*0.001*
cv_A2*A2	*0.001*
cv_A3*A3	*0.001*
Mean r	*0.991*

We conclude that the interannual variability of amplitude is not negligible (Figure 4) but much smaller than mean *r (Table 1)*. Because of the latter, the main values of the Fourier components over the period from 2000 to 2006 were used to characterize the annual temporal profile of the pixel-wise ratio.

Correlation between air temperature and surface temperature was evaluated by linear regression analysis. We found high correlations with R2 values greater than 0.8. The resulting parameters of linear functions are m_0=1.18, n_0=-52.11, m_1=0.81, n_1=58.76.

Air temperature was calculated and validated against observations at four stations from 2000 to 2005. RMSE varied between 3.2 K and 3.9 K for daily maximum temperature. Smaller RMSE values were obtained for the 5 and 10 days moving averages (Table. 2).

Table 2. RMSE in Ta estimation at four stations in Valle Telesina area evaluated from 2000 to 2005.

	RMSE	***RMSE 5 Days moving average***	***RMSE 10 Days moving average***
	Daily (K)	Average (K)	Average (K)
Solopaca	3.9	1.7	1.5
Castelvenere	3.6	2.0	1.7
Guardia Sanframondi	3.6	2.1	2.0
Telese	3.2	1.9	1.9

We obtained comparable RMSE values when evaluating our method against the fully independent daily air temperature data observed at Benevento station from 1984 to 1988 (RMSE=2.8 K).

DISCUSSION

We have applied HANTS as described above to remove cloud contaminated observations and we used three harmonic components. To evaluate this solution we tested several combinations of parameters where the number of frequencies and FET were changed. Negative outliers e.g. due to clouds, are identified as that observations deviating from the curve fitting in the lower direction. The FET value relates to the difference in brightness temperature between the land surface and a cloud top.

The use of an increasing number of frequencies reduces the accuracy in the reconstruction of the land surface temperature by HANTS reproducing a not realistic temporal trend. In Figure 3 is shown an example obtained by using three different number of frequencies and setting the FET parameter to 5 K and to 8 K. We observe that the typical temporal trend is well reproduced by using tree frequencies while increasing number of frequency causes a false sharply increasing or decreasing temporal trend in some periods of time. This is especially evident when gaps are present in association with not accurate measurements (retrievals). In the latter case the difficulty in determining the cause of the dispersion of measurements (this could be due to errors in LST retrieval or for example to sensor noise) does not assure a good accuracy of reconstructed Land Surface Temperature.

A further consideration is that, since we use the model of the time series as a reference at each iteration, the deviation of an observation depends from the model itself, besides objective causes. The interaction between model structure (i.e. the frequencies used) and fitting error is documented by fitting the same data with three, five and seven harmonic components. The fitting error decreases with increasing number of frequencies, as expected. When using five and seven

frequencies, evident artefacts appeared and we focused on evaluating the three frequency solution (Fig.5a and 5d). The use of additional harmonics allows a closer fitting to shorter fluctuations, but in some case (see detail inset Fig.5b, 5c, 5e and 5f), this seems to generate artefacts like e.g. a secondary modes in the time series, which seems to be due to noise rather than to the underlying signal.

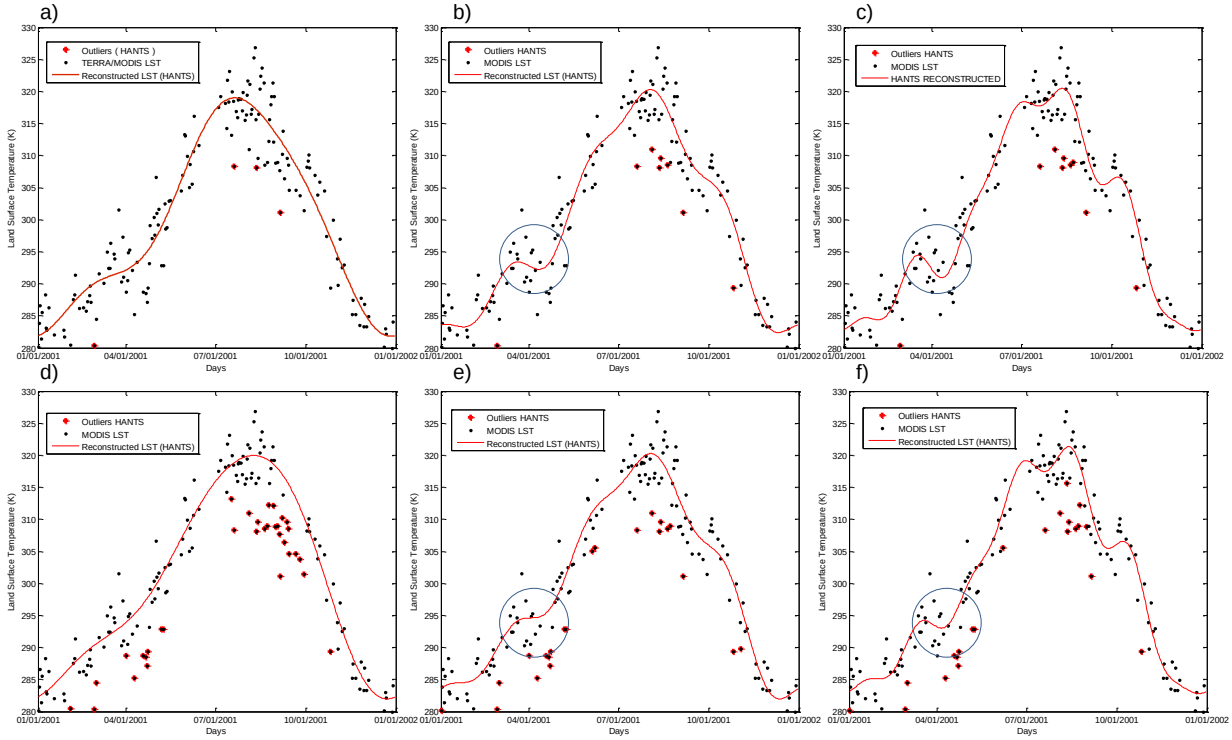

Figure 5. Reconstruction of LST by HANTS algorithm at one location using different combination of parameters FET and frequencies (f). a) FET=8, f=3; b)FET=8, f=5; c) FET=8, f=7; d)FET=5, f=3; e) FET=5, f=5; f) FET=5, f=7.Green points: LST measurements; red crosses: outliers identifyed by HANTS; red line: Reconstructed LST

The use of a FET = 5 K seems to return the best reconstruction of the land surface temperature (Figure 4.d). This choice was also suggested by Julien et al, 2006 (13) for cloud removal in LST time series.

We have also evaluated (Figure 6) whether the outliers identified by our method do match the ones identified by the quality flag of MODIS LST data. In this case we remove positive and negative outliers in two consecutive steps. In the first we use all data in the time series to remove negative outliers e.g. due to cloud (as explained above). In a second step, positive outliers e.g. due to retrieval errors are removed applying HANTS to the remaining data after removal of the negative outliers. In a number of cases, i.e. where open circles and crosses do not coincide, our procedure detects outliers not identified by the MODIS quality flag, while all outliers identified by the quality flag (QA = 1) are also identified by our method.

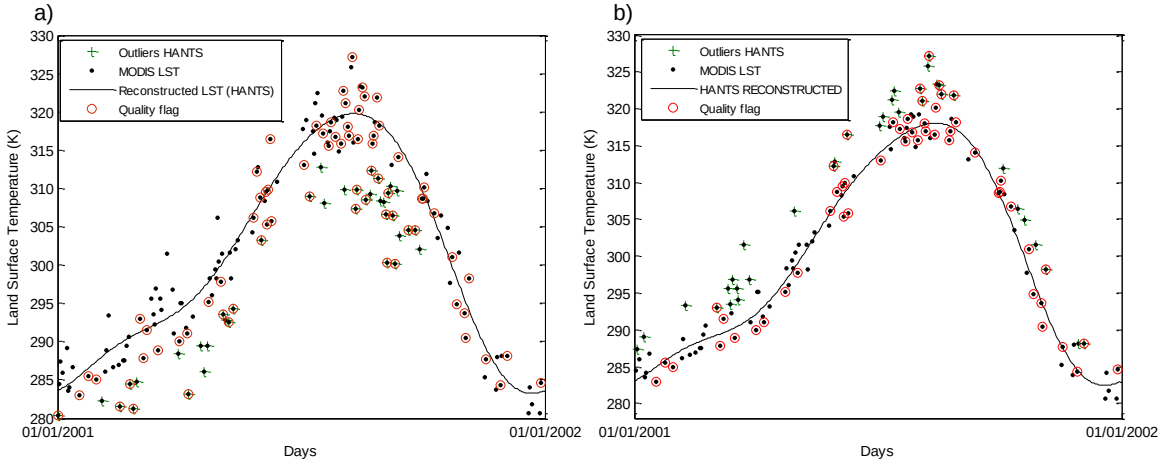

Figure 6. Removal of negative (a) and positive (b) outliers and gap filling using HANTS algorithm. Removed outliers (green crosses) are compared with MODIS Quality Assessment code (red circles= Mandatory QA flag 01).

The *r* values are controlled by morphology, land cover and hydrological conditions. An example of the variability is illustrated in Figure 7 and the characteristics of these four sites are given in Table 3. The *r* values are generally lower than one because the reference location is an urban area. The r values at Location 2 are lower than the ones at location 3 because of the higher elevation, everything else being nearly the same. The north facing forest patch at location 4 has lower r values that the south facing forest patch at location 2 at similar elevation. The r values at location 1 are occasionally higher than one because this is a non irrigated patch of agricultural land, presumably very dry in summer.

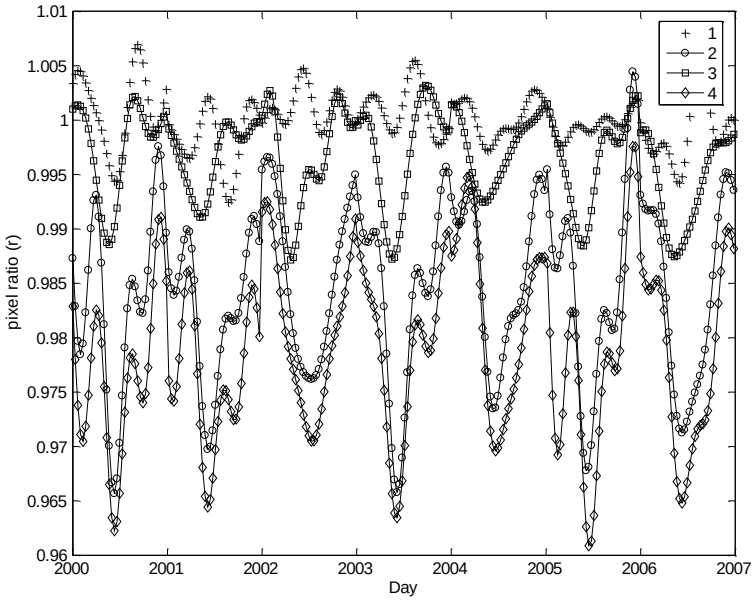

Figure 7.Temporal trends of r ratio at four different locations in Valle Telesina area

The comments above suggest that the accuracy of the estimated air temperature could be further improved by applying a smaller error tolerance, say FET < 5 K, while the use of limiting the number of harmonics has been correct. The interpretation of differences in the yearly pattern of r suggest interesting ideas for further analyses of the relation between morphology, land cover and the difference between surface and air temperature

Table 2. Morphological and land cover attributes of five locations in the Valle Telesina; locations 1 through 4 are the same as in Figure 7

Location	Lat (°)	Lon (°)	Esposure (°)	Slope (°)	Altitude (m)	Land Cover (CORINNE 2000)
1	14.44	41.13	26.75	1.37	47	Agricultural areas,Arable land,Non-irrigated arable land
2	14.54	41.13	243.11	19.97	641	Forest and semi natural areas,Forests,Broad-leaved forest
3	14.41	41.23	351.14	12.85	181	Forest and semi natural areas,Forests,Broad-leaved forest
4	14.55	41.15	111.50	18.08	543	Forest and semi natural areas,Forests,Broad-leaved forest
Reference	14.48	41.23	221.73	3.01	94	Artificial surfaces,Urban fabric,Discontinuous urban fabric

CONCLUSIONS

Our method does provide a significant improvement in the spatial resolution of air temperature observations and, more importantly, the model of spatial and temporal variability of air temperature is applicable to a period of time different from the one of model construction. The latter has been evaluated by using past observations of air temperature, which justifies the use of the model to downscale future climate scenario.

The selection of HANTS parameters did require as usual some initial trial and error, but the values we used led to estimates of air temperature with accuracy comparable with the estimated LST retrieval error. As expected, the error decreased when considering 5 and 10-days moving averages, which is promising in view of further investigations on the response of plant phenology to climate.

ACKNOWLEDGEMENTS

The work was carried out within the Italian national project AGROSCENARI funded by the Ministry for Agricultural, Food and Forest Policies (MIPAAF, D.M. 8608/7303/2008)

REFERENCES

1 Prihodko L. and S N Goward, 1997. Estimation of Air Temperature from Remotely Sensed Surface Observations. Remote Sensing of the Environment, 60: 335-346.

2 Nemani R R & Running S W,1997. Land cover characterization using multitemporal red, near-IR, and thermal-IR data from NOAA/AVHRR. Ecological Applications, 7(1): 79−90.

3 Vacutsem, C., P Ceccato, T Dinku, S J Connor, 2010. Evauation of MODIS land surface temperature data to estimate air temperature in different ecosystems over Africa. Remote Sensing of Environment, 114: 449-465.

4 Jones P., G. Jedlovec, R Suggs & S Haines, 2004. Using MODIS LST to estimate minimum air temperature at night. In: 13th Conference on Satellite Metereology and Oceanography, (American Metereological Society, Norfolk, Virginia) 6pp.

5 Gallo K, R Hale, D Tarpley, Y Yu, 2011. Evaluation of the Relationship between Air Temperature and Land Surface Temperature under Clear- and Cloudy-Sky Condition. Journal of Applied Meteorology and Climatology, 50(3): 767-775.

6 Hengl T, G B M Heuvelink, M Perčec Tadić, E J Pebesma, 2012. Spatio-temporal prediction of daily temperatures using time-series of MODIS LST images. Theor Appl Climatol, 107: 265–277.

7 Cresswell MP, AP Morse, MC Thomson, SJ Connor, 1999. Estimating surface air temperatures, from Meteosat land surface temperatures, using an empirical solar zenith angle model. Int J Remote Sensing, 20: 1125–1132.

8 Stisen S, Sanholt I, Norgaard A, Fensholt R, Eklundh L, 2007. Estimation of diurnal air temperature using MSG SEVORI data in West Africa. Remote Sensing of Environment, 110: 262-274.

9 Mostovoy G., King R., Reddy K., Kakani V. and Filippova, M, 2006. Statistical estimation of daily maximum and minimum air temperatures from MODIS LST over the State of Mississipi. GIScience & Remote Sensing, 43: 78:110.

10 Wan Z., Zhang Y, Zhang Q, and LI Z L, 2002b. Validation of the land-surface temperature products retrieved from Terra Moderate Resolution Imaging Spectroradiometer data. Remote Sensing of Environment, 83: 163–180.

11 Menenti M., Azzali S, Verhoef W, and van Swol R, 1993. Mapping agroecological zones and time lag in vegetation growth by means of Fourier analysis of time series of NDVI images. Adv. Space Res.,13(5): 233–237.

12 Verhoef W, Menenti M, and Azzali S, 1996. A colour composite of NOAA–AVHRR–NDVI based on time series analysis (1981–1992). International Journal of Remote Sensing, 17(2): 231–235.

13 Julien Y, Sobrino J A, Verhoef W, 2006. Changes in land surface temperatures and NDVI values over Europe between 1982 and 1999. Remote Sensing of Environment, 103 (2006) : 43 – 55.